

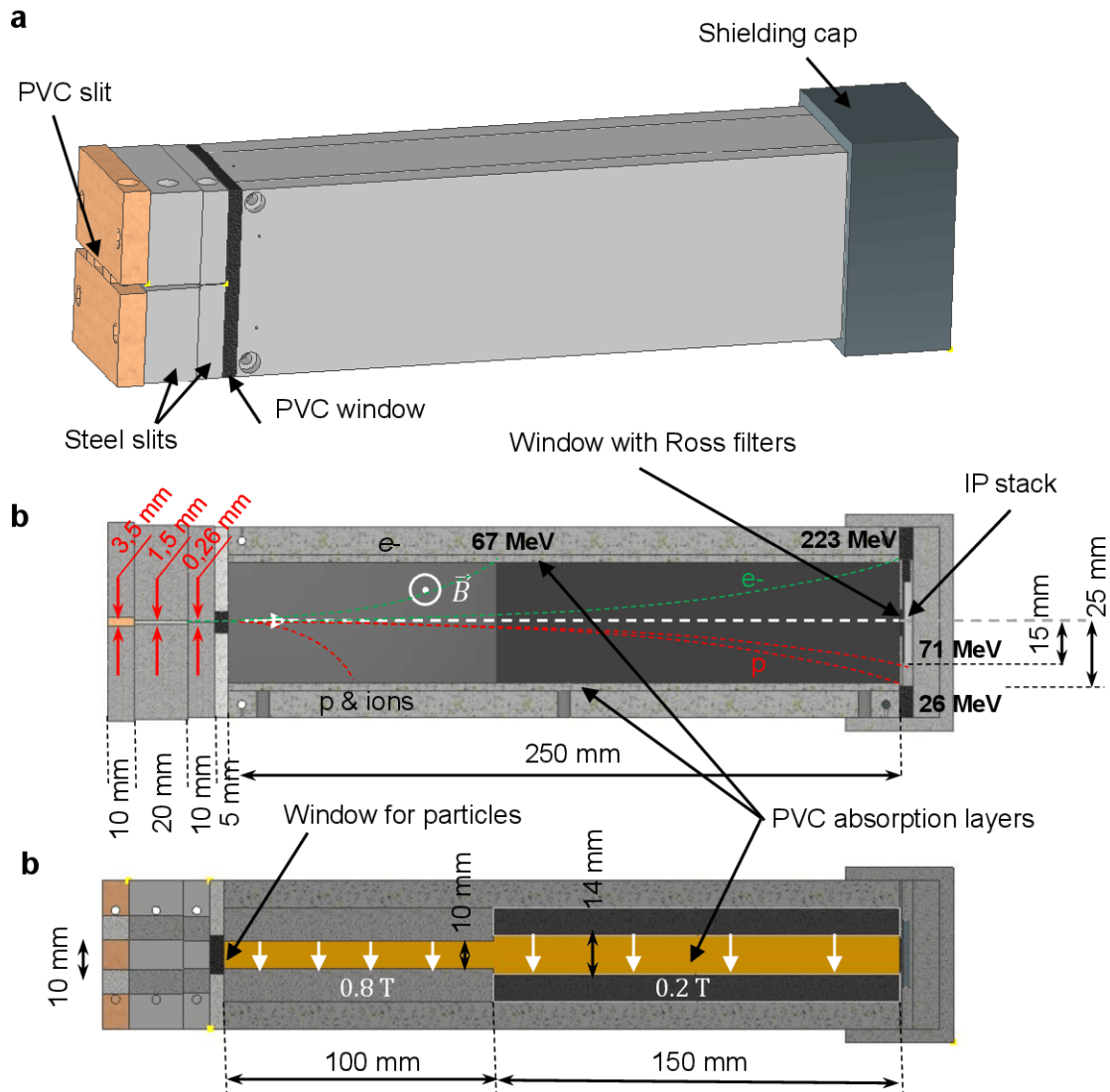
# 1 Supplementary Information

2

## 3 Description of X-MS, technical parameters

4 The modified magnetic spectrometer (Fig. 1S) incorporates several improvements that allow  
5 measuring X-ray radiation from laser-target interaction. It uses a set of stepped entrance slits  
6 to reduce background noise while also avoiding clipping of information from laterally distributed  
7 sources.

8



9

10 **Fig.1S: a.** Detailed drawing of the modified magnet spectrometer for X-ray radiation registration (X-  
11 MS). **b.** Side view of the X-MS, shown in a central vertical section. **c.** Top view of the X-MS, shown  
12 in a central horizontal section.

13

14 X-ray signal is registered on the wall of the X-MS opposite to the entrance slit, using a set  
15 of Ross filters followed by an IP-stack. Electrons with energies up to 220 MeV and protons with  
16 energies up to 70 MeV are deflected to the side by pairs of permanent magnets with strengths  
17 of 0.8 T and 0.2 T. Since particles of such high energy have not been observed in experiments,  
18 their influence on the registered X-ray signal can be excluded.

19

20 **Using Ross filter system for spectra evaluation**

21 Table 1S presents the main parameters of the used Ross filters, including material, thickness,  
 22 and K-edge energy.

23

24 **Table 1S.** Ross filter system in X-MS

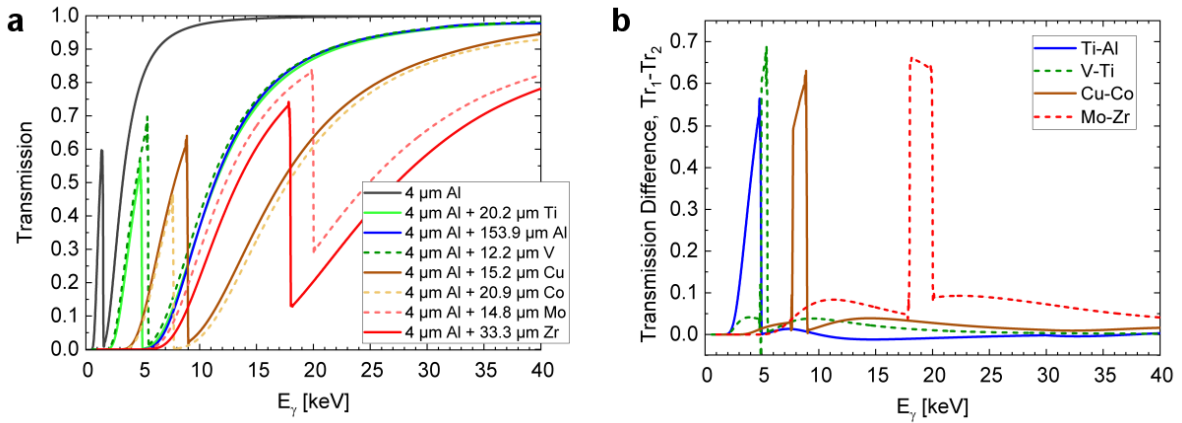
Filter 1				Filter 2				<E> [eV]	$\Delta E$ [eV]
Material	$d_1$ [ $\mu\text{m}$ ]	$\Delta d_1$ [ $\mu\text{m}$ ]	$E_1$ [eV]	Material	$d_2$ [ $\mu\text{m}$ ]	$\Delta d_2$ [ $\mu\text{m}$ ]	$E_2$ [eV]		
Ti	20.2	0.7	4966	Al	153.9	1.4	1560	3263	1703
V	12.2	0.9	5482	Ti	20.2	0.9	4966	5224	258
Cu	15.2	1.0	8979	Co	20.9	1.7	7710	8345	635
Mo	14.8	0.7	20000	Zr	33.3	1.1	17998	18999	1001

25

26

27 The image of the Ross filter system consisting of seven filters is shown in Fig. 5a, "Methods".  
 28 Prior to Ross filters, the radiation undergoes attenuation in a 4  $\mu\text{m}$  aluminum foil, which serves  
 29 as an overall filter to reduce the intensity of soft X-rays below 0.5 keV (characteristic radiation  
 30 of CHO-plasma). The transmission of the filters and the transmission difference for the Ross  
 31 filter pairs are shown in Fig. 2S a and b, respectively.

32



33

34

35 **Fig. 2S:** a. Transmission of the applied filter. b. Transmission difference for Ross filter pairs.

36

37 The evaluation procedures begin with the general representation of the signal difference  
 38 after the Ross filter pair:

$$39 \quad S_i - S_j = \theta_z \int_0^{+\infty} f_\gamma(E) \cdot \Delta\Omega \cdot (Tr_i(E) - Tr_j(E)) \cdot S_{IP}(E) \cdot dE, \quad (1)$$

40 Here,  $S_i, S_j$  represents the signal [PSL/px] on the IP after the i-th filter,  $\theta_z$  is the fading factor  
 41 of IP signal,  $f_\gamma(E)$  is the photon energy distribution function,  $\Delta\Omega$  is the solid angle of observation  
 42 of the X-ray source on the IP within one pixel ( $\Delta\Omega = \left(\frac{l_{1px}}{L_{IP}}\right)^2$ , where  $L_{IP}$  is the distance between  
 43 the X-ray source and the IP detector after the filter, and  $l_{1px}$  is the size of one pixel on the IP),  
 44  $Tr_i(E) \cdot S_{IP}(E)$  is the product of the transmission of the i-th filter and the IP sensitivity.

45 Since  $Tr_i(E) - Tr_j(E)$  differs from zero only within the energy window from  $E_1$  to  $E_2$ , an  
 46 approximation can be used for the general expression (1):

$$47 \quad S_i - S_j \cong \theta_z \int_{E_1}^{E_2} f_\gamma(E) \cdot \Delta\Omega \cdot (Tr_i(E) - Tr_j(E)) \cdot S_{IP}(E) \cdot dE. \quad (2)$$

48

49 Furthermore, assuming that the distribution function  $f_\gamma$  within the energy interval from  $E_1$  to  
50  $E_2$  changes insignificantly, the following approximation holds:

$$51 \quad f_{\gamma 0} = f_{\gamma 0}|_{E_1, E_2} \cong \frac{S_i - S_j}{\theta_z \cdot \Delta\Omega \cdot \int_{E_1}^{E_2} (Tr_i(E) - Tr_j(E)) \cdot S_{IP}(E) \cdot dE}. \quad (3)$$

52 Therefore, it is possible to estimate different points in the X-ray spectrum using equation  
53 (3). Due to the approximation (3), the error of the method increases. However, the use of the  
54 estimation (3) allows for a "zero approximation" of the photon distribution function to be ob-  
55 tained.

56 Since the transmission difference of the Ross filter pair is non-zero outside the energy win-  
57 dows, an error arises in the Ross filter method. To reduce this error, a calculation correction can  
58 be applied to the Ross filter method. The values obtained through equation (3) can be regarded  
59 as the values of the distribution function in a "zero-approximation". For a more accurate calcu-  
60 lation, it is necessary to use the original general equation (1).

$$61 \quad S_i - S_j = \theta_z \int_0^{+\infty} f_\gamma(E) \cdot \Delta\Omega \cdot (Tr_i(E) - Tr_j(E)) \cdot S_{IP}(E) \cdot dE, \quad (4)$$

62 or

$$63 \quad S_i - S_j = I_1 + I_2 + \theta_z \int_{E_1}^{E_2} f_\gamma(E) \cdot \Delta\Omega \cdot (Tr_i(E) - Tr_j(E)) \cdot S_{IP}(E) \cdot dE \quad (5)$$

64 with

$$65 \quad I_1 = \theta_z \int_0^{E_1} f_\gamma(E) \cdot \Delta\Omega \cdot (Tr_i(E) - Tr_j(E)) \cdot S_{IP}(E) \cdot dE, \quad (6)$$

$$66 \quad I_2 = \theta_z \int_{E_2}^{+\infty} f_\gamma(E) \cdot \Delta\Omega \cdot (Tr_i(E) - Tr_j(E)) \cdot S_{IP}(E) \cdot dE \quad (7)$$

67 Furthermore, equation (5) is used for an iterative calculation of the desired distribution func-  
68 tion  $f_\gamma$ . In the correction terms  $I_1$  and  $I_2$ , the "zero-approximation function"  $f_{\gamma 0}$  is employed,  
69 while in the remaining integral, the function  $f_\gamma$  is taken out of the integral under the assumption  
70 that the distribution function  $f_\gamma$  undergoes negligible changes in the energy interval from  $E_1$  to  
71  $E_2$ . Consequently, it is possible to compute the "first-approximation function"  $f_{\gamma 1}$ .

$$72 \quad f_{\gamma 1} = f_{\gamma 1}|_{E_1, E_2} \cong \frac{S_i - S_j - I_{10} - I_{20}}{\theta_z \cdot \Delta\Omega \cdot \int_{E_1}^{E_2} (Tr_i(E) - Tr_j(E)) \cdot S_{IP}(E) \cdot dE} \quad (8)$$

73 with

$$74 \quad I_{10} = \theta_z \cdot \Delta\Omega \int_0^{E_1} f_{\gamma 0}(E) \cdot (Tr_i(E) - Tr_j(E)) \cdot S_{IP}(E) \cdot dE, \quad (9)$$

$$75 \quad I_{20} = \theta_z \cdot \Delta\Omega \int_{E_2}^{+\infty} f_{\gamma 0}(E) \cdot (Tr_i(E) - Tr_j(E)) \cdot S_{IP}(E) \cdot dE. \quad (10)$$

76 The iterative calculations can be continued for the k-th iteration as follows:

$$77 \quad f_{\gamma, k} = f_{\gamma, k}|_{E_1, E_2} \cong \frac{S_i - S_j - I_{1, k-1} - I_{2, k-1}}{\theta_z \cdot \Delta\Omega \cdot \int_{E_1}^{E_2} (Tr_i(E) - Tr_j(E)) \cdot S_{IP}(E) \cdot dE} \quad (11)$$

78 with

$$79 \quad I_{1, k-1} = \theta_z \cdot \Delta\Omega \int_0^{E_1} f_{\gamma, k-1}(E) \cdot (Tr_i(E) - Tr_j(E)) \cdot S_{IP}(E) \cdot dE \quad (12)$$

$$80 \quad I_{2, k-1} = \theta_z \cdot \Delta\Omega \int_{E_2}^{+\infty} f_{\gamma, k-1}(E) \cdot (Tr_i(E) - Tr_j(E)) \cdot S_{IP}(E) \cdot dE. \quad (13)$$

81 The completion of the calculations can be defined by a condition for the difference between  
82 the previous and new iterative distribution functions, for example,  $\delta < 0.05$  (5%), where:

$$83 \quad \delta \equiv \max(\delta_l) \text{ where } \delta_l = \left| 1 - \frac{f_{\gamma, k-1}(E_l)}{f_{\gamma, k}(E_l)} \right| \quad (14)$$

84 Here,  $E_l = \frac{E_1 + E_2}{2}$  represents the average energy in the energy window from  $E_1$  to  $E_2$  for the  
 85  $l$ -th Ross filter pair used. The calculations can be automated using a Python code.

86

### 87 Using multi-IP-filters for spectra evaluation

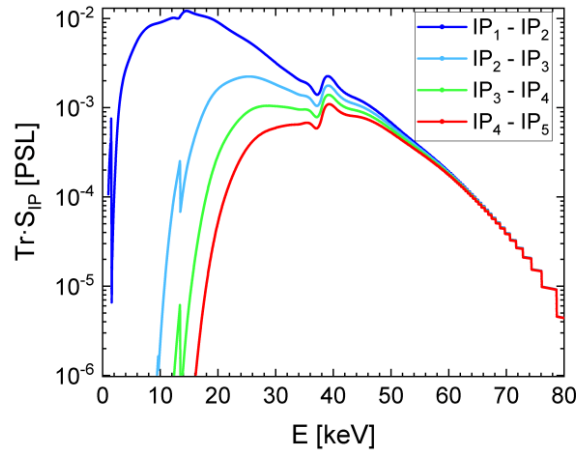
88 Furthermore, it is possible to obtain additional data points in the spectrum (for high-energy X-  
 89 rays) from the measurements of the X-ray signal by the stack of five IPs (Fig. 5a). For this  
 90 purpose, the Differential Averaged Transmission (DAT) method<sup>8</sup> was used. This method is  
 91 based on the maximum signals measured on the IP series ( $M_1, M_2, M_3, M_4, M_5$ ):

$$92 \quad M_i = \theta_z \int f_\gamma(E) \cdot \Delta\Omega \cdot Tr_i(E) \cdot S_{IP}(E) \cdot dE. \quad (15)$$

93 Then, the difference between the signals in two adjacent IPs is given by:

$$94 \quad M_i - M_j = \theta_z \int f_\gamma(E) \cdot \Delta\Omega \cdot (Tr_i(E) - Tr_j(E)) \cdot S_{IP}(E) \cdot dE. \quad (16)$$

95 Here, the product of the transmission difference and IP sensitivity  $(Tr_i(E) - Tr_j(E)) \cdot S_{IP}(E)$   
 96 depends on the photon energy (Fig. 3S).



97

98 **Fig. 3S.** Dependence of the product of the transmission difference and IP sensitivity on photon  
 99 energy for the IP pairs in the consecutive IPs.

100 For the calculations, the transmission data from the source<sup>60</sup>: [https://henke.lbl.gov/opti-](https://henke.lbl.gov/optical_constants/)  
 101 [cal\\_constants/](https://henke.lbl.gov/optical_constants/) were used for photon energies ranging from 0.5 to 30 keV. For higher energies,  
 102 the transmission is calculated using the data of the mass attenuation coefficient ( $\mu/\rho$ ) and the  
 103 density of the filter material  $\rho$  from the source<sup>61</sup>: [https://physics.nist.gov/PhysRefData/Xray-](https://physics.nist.gov/PhysRefData/Xray-MassCoef/tab3.html)  
 104 [MassCoef/tab3.html](https://physics.nist.gov/PhysRefData/Xray-MassCoef/tab3.html), according to the formula:

$$105 \quad Tr = \exp\left(-\frac{\mu}{\rho} \rho d\right), \quad (17)$$

106 where  $d$  is the thickness of the filter. If the filter consists of multiple  $n$  layers, the formula is  
 107 given by:

$$108 \quad Tr = \prod_{k=1}^n (Tr_k) = \exp\left(-\sum_{k=1}^n \left(\frac{\mu_k}{\rho_k} \rho_k d_k\right)\right). \quad (18)$$

109 Here,  $k$  is the index of a filter layer. The sensitivity  $S_{IP}(E)$  of BAS-IP MS was taken from<sup>56,62</sup>.

110 From equation (16), an approximation for the measurements in  $IP_1$  and  $IP_2$  can be derived:

$$111 \quad M_1 - M_2 \cong f_\gamma \Big|_{E_{12}} \cdot \theta_z \cdot \Delta\Omega \int_{E_1}^{E_2} (Tr_1(E) - Tr_2(E)) \cdot S_{IP}(E) \cdot dE \quad (19)$$

112 with the restrictions  $E_1$  and  $E_2$ , which are half of the maximum value of  $(Tr_1(E) - Tr_2(E)) \cdot$   
113  $S_{IP}(E)$ .

114 Therefore,  $f_\gamma|_{E_{12}}$  can be calculated as:

$$115 \quad f_\gamma|_{E_{12}} \cong \frac{M_1 - M_2}{\theta_z \cdot \Delta\Omega \int_{E_1}^{E_2} (Tr_1(E) - Tr_2(E)) \cdot S_{IP}(E) \cdot dE}. \quad (20)$$

116 and for  $IP_2$  and  $IP_3$ :

$$117 \quad f_\gamma|_{E_{23}} \cong \frac{M_2 - M_3}{\theta_z \cdot \Delta\Omega \int_{E_2}^{E_3} (Tr_2(E) - Tr_3(E)) \cdot S_{IP}(E) \cdot dE} \quad (21)$$

118 The calculation according to equations (20) and (21) can be performed using a Python code.

119 Thus, the distribution function  $f_\gamma$  is determined by  $f_\gamma|_{E_{12}}$ ,  $f_\gamma|_{E_{23}}$  etc.

120 The error in energy corresponds to the energy window where the value of the product  
121  $(Tr_j(E) - Tr_i(E)) \cdot S_{IP}(E)$  for the  $ij$ -IP-pair is  $\geq 50\%$  of the maximum value (see Fig. 3S). The  
122 systematic error of 20–30% for the number of photons/keV/sr can be roughly estimated by  
123 contribution of the signal outside the energy window. The statistical error reaches 10 to 20%  
124 as a result of signal noise on the IPs.

125

126

127

128

## 129 References

130 60. Henke, B.L. *et al.* X-ray interactions: photoabsorption, scattering, transmission, and  
131 reflection at  $E = 50$ -30000 eV,  $Z=1$ -92. *Atomic Data and Nuclear Data Tables*. **54(2)**, 181-342.  
132 [https://henke.lbl.gov/optical\\_constants/](https://henke.lbl.gov/optical_constants/) (1993).

133 61. Hubbell, J.H. and Seltzer, S.M. X-Ray Mass Attenuation Coefficients (NIST Standard  
134 Reference Database 126). <https://www.nist.gov/pml/x-ray-mass-attenuation-coefficients>  
135 (1996).

136 62. Boutoux, G. *et al.* Validation of modelled imaging plates sensitivity to 1-100 keV x-rays  
137 and spatial resolution characterisation for diagnostics for the "PETawatt Aquitaine Laser". *Rev.*  
138 *Sci. Instrum.* **87**, 043108. <http://dx.doi.org/10.1063/1.4944863> (2016).